Analysis of nuclear structure effects in sub-barrier fusion dynamics using energy dependent Woods-Saxon potential

M. Singh Gautam
Department of Physics, Indus Degree College,
Kinana, Jind-126102 (Haryana), India
e-mail: gautammanjeet@gmail.com

Received 4 January 2016; accepted 15 April 2016

The fusion dynamics of various projectiles ($^{16}_{8}$O, $^{27}_{13}$Al and $^{37}_{17}$Cl) with the $^{70,72}_{32}$Ge-isotopes is analyzed using the energy dependent Woods-Saxon potential model (EDWSP model) and the coupled channel formulation. The impacts of the inelastic surface excitations of fusing nuclei have been examined using the coupled channel model and by inclusion of appropriate number of the intrinsic channels, the observed fusion enhancements can be reasonably explained for all fusing systems. The magnitude of the sub-barrier fusion enhancement is found to be increasing with the increase of deformation parameter associated with the colliding systems. Furthermore, the optimum choice of the static Woods-Saxon potential and the EDWSP model are simultaneously tested along with the Wong's approximation for explanation of the fusion of $^{16}_{8}$O + $^{70,72}_{32}$Ge, $^{27}_{13}$Al + $^{70,72}_{32}$Ge and $^{37}_{17}$Cl + $^{70,72}_{32}$Ge reactions. The theoretical predictions obtained by using the static Woods-Saxon potential model are found to be substantially smaller than the experimental data particularly at below barrier energies. In contrast, the EDWSP model based calculations provide an adequate description of the observed fusion enhancement of the chosen reactions. This unambiguously reveals that the discrepancies between theoretical results obtained through the single barrier penetration model and the experimental data can be partially or fully removed if either one makes the use of the EDWSP model along with the Wong's approximation or includes the intrinsic channels associated with the fusing systems in coupled channel calculations. In addition, the EDWSP model based predictions are capable of recovering an agreement with the fusion data within 10%. For chosen reactions, only at 7 fusion data points out of 77 fusion data points does the deviation exceed 5% while 70 fusion data points lie within 5%. Therefore, the EDWSP model based calculations are able to provide close agreement with the fusion data points at above barrier energies within 5% with a probability more than 90%.

Keywords: Heavy-ion near-barrier fusion reactions; coupled channel equations; Woods-Saxon potential; diffuseness anomaly.

PACS: 25.60.Pj; 21.60.Ev; 24.10.Eq

1. Introduction

In the past few decades, the large number of theoretical and experimental efforts has been concentrated to investigate the role of the nuclear structure degrees of freedom of collision partners on fusion process. The fusion reactions, wherein the colliding nuclei leads to the formation of a compound nucleus either by overcoming or by quantum mechanical tunneling through the Coulomb barrier, have emerged as one of the most sensitive nuclear spectroscopic tool to examine the role of the nuclear structure of the participating nuclei as well as their nuclear interactions [1-3]. Despite of the lots of investigations done so far, the dynamics of fusion reactions still shows unexpected facets and attracts researcher to explore many unexplored features. Many theoretical and experimental evidences showed that the sub-barrier fusion excitation function data of various fusing systems is dramatically enhanced over the predictions of the one-dimensional barrier penetration model. Such fusion enhancement at near and sub-barrier energies has an intimate link with the nuclear structure degrees of freedom such as permanent deformation (deformed nuclei), vibration of nuclear surface (spherical nuclei), rotations of nuclei during collision, neck formation and nucleon (multi-nucleon) transfer reactions [1-4]. The coupling of such dominant intrinsic channels to the relative motion of the collision partners effectively reduces the interaction barrier between the colliding systems and consequently results in an anomalously large fusion excitation functions at below barrier energies. Within the coupled channel approach, the effect of inclusion of intrinsic channels associated with the colliding systems is to replace the nominal Coulomb barrier by a distribution of barriers of different height and weight. In barrier distribution, the presence fusion barriers whose heights are smaller than the Coulomb barrier allow the passage of flux from entrance channel to fusion channel and hence coupled channel calculations are capable of reproducing the observed fusion dynamics [5-6].

In theoretical description, the influences of the relevant intrinsic channels are incorporated through the nucleus-nucleus potential. In this respect, the choice of nuclear potential is very crucial in order to judge the success of the theoretical approach. In heavy ion fusion reactions, the optimum choice of the nucleus-nucleus potential, which consists of the Coulomb repulsive interaction, centrifugal term and short range attractive nuclear potential, strongly affects the magnitude of fusion excitation functions and hence an accurate knowledge with regard the nuclear potential greatly simplifies the problem of understanding of the basic mechanism involved in the nuclear reaction dynamics [7-20]. The nuclear potential of the Woods-Saxon form, wherein the depth, range and diffuseness parameters are interrelated, is often used to preview the various features of the heavy ion colli-

sions. For this potential, the different sets of potential parameters are associated with different nuclear interactions between the collision partners. In case of elastic scattering analysis, a diffuseness of $a = 0.65\ fm$ is the most suitable for good description of the data. In contrast to this, a much larger value of the diffuseness parameter ranging from $a = 0.75\ fm$ to $a = 1.5\ fm$ has been extracted from the systematics of the fusion reactions [21-23]. This diffuseness anomaly, which might preview the various static and dynamical physical effects, is one of the interesting and challenging issue of heavy ion collisions. For heavy ion reactions, the recent analysis [16,24-28] suggested that the energy dependence in nucleus-nucleus potential is another essential feature of nuclear potential. Such energy dependence is also pointed out in double folding potential wherein it originates from the nucleon-nucleon interactions as well as the non-local quantum effects. The non-local quantum effects are directly linked with the exchange of nucleons between the colliding systems and consequently generate a velocity dependent nuclear potential [16,24]. The energy dependence of the local equivalent potential is related to the finite range of Pauli nonlocality which in turn manifests the exchange of nucleons during nuclear interactions [16,24]. It is quite interesting to note that the energy dependence in nucleus-nucleus potential is also reflected from the microscopic time-dependent Hartree-Fock theory [25-28]. In Ref. 25 to 26, it has been shown that in the domain of the Coulomb barrier, the nuclear potential becomes energy dependent and such energy dependence occurs due to coordinate-dependent mass and the involvement channel coupling effects associated with the collision partners. In this sense, the energy dependent nuclear potential may give better explanation of the many uncharted features of nuclear interactions. To include nuclear structure effects as well as the energy dependence in nucleus-nucleus potential, the earlier work undertook several efforts by introducing the energy dependence in the Woods-Saxon potential via its diffuseness parameter [29-31].

In this work, the fusion dynamics of $^{16}_{8}$O + $^{70,72}_{32}$Ge, $^{27}_{13}$Al + $^{70,72}_{32}$Ge and $^{37}_{17}$Cl + $^{70,72}_{32}$Ge reactions [32-42] is analyzed within the view of the static Woods-Saxon potential and the energy dependent Woods-Saxon potential model (EDWSP model) [4,8-9,13,17-18,29-31] along with the Wong's approximation [43]. As far as the colliding systems are concerned, the projectiles exhibit dominance of the different nuclear structure degrees of freedom and consequently results in the different energy dependence of the sub-barrier fusion cross-sections. The lighter projectile ($^{16}_{8}$O) is spherical nucleus, wherein the low lying inelastic surface excitations are dominant mode of couplings. The heavier projectiles ($^{27}_{13}$Al and $^{37}_{17}$Cl) are oblate in shape but due to odd-A nature possess large number of low lying inelastic surface excitations and coupling to such vibrational states produces substantially larger sub-barrier fusion enhancement over the predictions of the one dimensional barrier penetration model. Furthermore, $^{16}_{8}$O-isotope is doubly magic, $^{27}_{13}$Al-isotope is non-magic while the $^{37}_{17}$Cl-isotope is magic nucleus and hence fusion dynamics of different projectiles ($^{16}_{8}$O, $^{27}_{13}$Al and $^{37}_{17}$Cl) with the $^{70,72}_{32}$Ge-isotope provides more concrete statement about the influences of internal degrees of freedom on fusion process. In case of target isotopes ($^{70,72}_{32}$Ge), which are spherical in shape, the inelastic surface excitations play very crucial role in sub-barrier fusion dynamics. The theoretical calculations based on the static Woods-Saxon potential are unable to explain the observed fusion dynamics of the chosen reactions. Such discrepancies between theoretical predictions and the below barrier fusion data can understood in terms of the collective excitations of collision partners. The inclusions of the dominant intrinsic channels in coupled channel calculations, which are performed using the code CCFULL [44], overcome these deviations. In contrast, the energy dependence in nucleus-nucleus potential introduces various kinds of barrier modifications and consequently reduces the fusion barrier which in turn responsible for the predictions of larger sub-barrier fusion excitation functions with reference to the simple one dimensional barrier penetration model. The brief description of the method of calculation is given in Sec. 2. The results are discussed in detail in Sec. 3 while the conclusions drawn are presented in Sec. 4.

2. Theoretical Formalism

2.1. Single channel description

The total fusion cross-section within the framework of partial wave analysis is defined as

$$\sigma_F = \frac{\pi}{k^2}\sum_{\ell=0}^{\infty}(2\ell+1)T_\ell^F \tag{1}$$

Hill and Wheeler proposed an expression for tunneling probability (T_ℓ^F), which is based on the parabolic approximation [45]. In parabolic approximations, the effective interaction potential between the collision partners has been replaced by a parabola and the tunneling probability through this barrier can be estimated by using the following expression.

$$T_\ell^{HW} = \frac{1}{1+\exp\left[\frac{2\pi}{\hbar\omega_\ell}(V_\ell - E)\right]} \tag{2}$$

This parabolic approximation was further simplified by Wong using the following assumptions for barrier position, barrier curvature and barrier height [43].

$$R_\ell = R_{\ell=0} = R_B \tag{3}$$

$$\omega_\ell = \omega_{\ell=0} = \omega \tag{4}$$

$$V_\ell = V_B + \frac{\hbar^2}{2\mu R_B^2}\left[\ell+\frac{1}{2}\right]^2 \tag{5}$$

with, V_B is the Coulomb barrier which corresponds to $\ell = 0$.

Using Eq. (2) to Eq. (5) into Eq. (1), the fusion cross-section can be written as

$$\sigma_F = \frac{\pi}{k^2}\sum_{\ell=0}^{\infty}\frac{(2\ell+1)}{\left[1+\exp\frac{2\pi}{\hbar\omega}(V_\ell - E)\right]} \tag{6}$$

By incorporating the contributions from the infinite number of partial waves to fusion process, one can change the summation over ℓ into integral with respect to ℓ in Eq. (6). By solving the integral one obtains the following expression of the one dimensional Wong formula [43].

$$\sigma_F = \frac{\hbar\omega R_B^2}{2E} \ln\left[1 + \exp\left(\frac{2\pi}{\hbar\omega}(E - V_B)\right)\right] \qquad (7)$$

In earlier work, the EDWSP model [4,8-9,13,17-18,29-31] successfully explores the fusion dynamics of various heavy ion fusion reactions wherein the inelastic surface excitations and nucleon (multi-nucleon) transfer channels are the most relevant intrinsic channels. This work examines the fusion mechanism of different projectiles ($^{16}_{8}$O, $^{27}_{13}$Al and $^{37}_{17}$Cl), which spans the dominance of different intrinsic channels, with common spherical targets ($^{70,72}_{32}$Ge). For theoretical predictions, the static Woods-Saxon potential and the energy dependent Woods-Saxon potential (EDWSP) model are exploited along with the one dimensional Wong formula. The coupled channel calculations are performed using the code CCFULL [44] wherein the static Woods-Saxon potential model has been used to entertain the influence of nuclear structure degrees of freedom of the fusing systems. In this sense, the optimum form of the static Woods-Saxon potential is defined as

$$V_N(r) = \frac{-V_0}{\left[1 + \exp\left(\frac{r-R_0}{a}\right)\right]} \qquad (8)$$

with $R_0 = r_0(A_p^{1/3} + A_T^{1/3})$. The quantities '$V_0$' is depth and '$a$' is diffuseness parameter of the Woods-Saxon potential. In EDWSP model, the depth of real part of the Woods-Saxon potential is defined as

$$V_0 = \left[A_p^{\frac{2}{3}} + A_T^{\frac{2}{3}} - (A_p + A_T)^{\frac{2}{3}}\right] \times \left[2.38 + 6.8(1 + I_p + I_T)\frac{A_p^{\frac{1}{3}} A_T^{\frac{1}{3}}}{A_p^{\frac{1}{3}} + A_T^{\frac{1}{3}}}\right] \text{ MeV} \qquad (9)$$

where

$$I_p = \left(\frac{N_p - Z_p}{A_p}\right)$$

and

$$I_T = \left(\frac{N_T - Z_T}{A_T}\right)$$

are the isospin asymmetry of fusing pairs.

In collision dynamics, the large number of static and dynamical physical effects occurs in the surface region of nuclear potential or tail region of the Coulomb barrier and consequently changes the parameters of nuclear potential. For instance, the variation of N/Z ratio of the colliding pairs, variation of surface energy and nucleon densities during nuclear interactions, the channel coupling effects like permanent deformation and low lying inelastic surface excitations of the colliding systems, nucleon (multi-nucleon) transfer channels, neck formation, dissipation of kinetic energy of the relative motion of the collision partners to their internal structure degrees or other static and dynamical physical effects generally occur in the tail region of the Coulomb barrier. These physical effects induce modifications in the values of the potential parameters and henceforth, results in the requirement of the different set of potential parameters for the different type of the nuclear interactions. In fusion dynamics, the diffuseness parameter of the static Woods-Saxon potential strongly alters the energy dependence of low energy fusion cross-section at near and below barrier energies and there is large number of experimental evidences wherein an abnormally large value of the diffuseness parameter is needed to explore the sub-barrier fusion data. The recently observed steep fall of fusion excitation function data at deep sub-barrier energy region in many medium mass nuclei, which is termed as fusion hindrance, can only be explained if one uses an abnormally large diffuseness parameter [2-3]. In addition, the nuclear structure effects present in surface region produce fluctuation in the strength of nuclear potential and this kind of fluctuation of nuclear strength is associated with the variation of the diffuseness parameter. It is worth noting here that the different channel coupling effects and non-local quantum effects which originate from the underlying nucleon-nucleon interactions induce the energy dependence in nucleus-nucleus potential. Therefore, to include all the above mentioned physical effects, the energy dependence in the Woods-Saxon potential was introduced via its diffuseness parameter. The energy dependent diffuseness parameter is defined as

$$a(E) = 0.85\left[1 + \frac{r_0}{13.75\left(A_p^{-\frac{1}{3}} + A_T^{-\frac{1}{3}}\right)\left(1 + \exp\left(\frac{\frac{E}{V_{B0}} - 0.96}{0.03}\right)\right)}\right] fm \qquad (10)$$

The range parameter (r_0) is an adjustable parameter and its value is optimized in order to vary the diffuseness parameter required to address the observed fusion dynamics of fusing system under consideration. In addition, the value of the range parameter (r_0) strongly depends on the nuclear structure of the participating nuclei and the type of dominance of nuclear structure degrees of freedom and hence the different set values of the range parameter (r_0) are required to explain the fusion dynamics of the different fusing systems. The po-

tential parameters (r_0, a and V_0) of the EDWSP model are interrelated and the change in one parameter automatically brings the corresponding adjustment in the values of other parameters. In the present model, the value of V_0 depends on the surface energy and isospin term of the interacting nuclei and the other two parameters (r_0 and a) are linked through the Eq. (10). Therefore, the values of the diffuseness parameter is directly related with the range parameter (r_0) which in turn geometrically defines the radii of the fusing systems ($R_0 = r_0(A_p^{1/3} + A_T^{1/3})$). Thus, the variation of the diffuseness parameter is directly linked with the fluctuation of radii of the colliding systems during their nuclear interaction. This consistency of the range parameter is also evident from the coupled channel models, wherein the radius parameter ($R_0 = r_0(A_p^{1/3} + A_T^{1/3})$) is used in the Woods-Saxon potential for incorporating the effects of the nuclear structure degrees of freedom of the fusing pairs [44,46-48]. The values of the range parameter used in the EDWSP model calculations for the chosen reactions are consistent with the commonly adopted values of the range parameter ($r_0 = 0.90\ fm$ to $r_0 = 1.35\ fm$), which are generally used in literature within the context of the different theoretical models for different colliding systems [1-3,5-6,48-49].

2.2. Coupled channel description

The coupled channel method that provides an adequate description of the fusion dynamics of various heavy on fusion reactions at near and sub-barrier energies is the most fundamental approach. In this method, the influences of intrinsic channels associated with the fusing systems are properly incorporated [44, 46-48]. In coupled channel approach, the following set of the coupled channel equation is solved numerically.

$$\left[\frac{-\hbar^2}{2\mu}\frac{d^2}{dr^2} + \frac{J(J+1)\hbar^2}{2\mu r^2} + V_N(r) + \frac{Z_P Z_T e^2}{r} + \varepsilon_n - E_{cm}\right]\psi_n(r) + \sum_m V_{nm}(r)\psi_m(r) = 0 \qquad (11)$$

where, $\bar{r}$ defines the radial separation between the interacting nuclei. μ is defined as the reduced mass of the colliding systems. E_{cm} and ε_n represent the bombarding energy in the center of mass frame and the excitation energy of the n^{th}channel respectively. V_{nm}, which consists of the Coulomb and nuclear components, is the matrix elements of the coupling Hamiltonian. The realistic coupled channel calculations are obtained within the view of the coupled channel code CCFULL [44]. In code CCFULL, the coupled channel equations are solved numerically by imposing the no-Coriolis or rotating frame approximation and ingoing wave boundary conditions (IWBC). The no-Coriolis or rotating frame approximation has been entertained for reducing the number of the coupled channel equations [44,46-48]. The ingoing wave boundary conditions (IWBC), which are quite sensitive to the existence of the potential pocket of the interaction fusion barrier, are well applicable for heavy ion collisions. According to IWBC, there are only incoming waves at the minimum position of the Coulomb pocket inside the barrier and there are only outgoing waves at infinity for all channels except the entrance channel. By incorporating the influence of the dominant intrinsic channels, the fusion cross-section can be written as

$$\sigma_F(E) = \sum_J \sigma_J(E) = \frac{\pi}{k_0^2}\sum_J (2J+1)P_J(E) \qquad (12)$$

where, $P_J(E)$ is the total transmission coefficient corresponding to the angular momentum J. The rotational coupling with a pure rotor and vibrational coupling in the harmonic limit are considered in the coupled channel approach. The rotational ($\hat{O}_R$) and vibrational couplings operator ($\hat{O}_V$) are defined as

$$\hat{O}_R = \beta_2 R_T Y_{20} + \beta_4 R_T Y_{40} \text{ and}$$
$$\hat{O}_V = \frac{\beta_\lambda}{\sqrt{4\pi}} R_T(a^\dagger_{\lambda 0} + a_{\lambda 0}) \text{ respectively.} \qquad (13)$$

where,R_T is defined as $r_{\text{coup}}A^{1/3}$, β_λ is the deformation parameter and $a^\dagger_{\lambda 0}(a_{\lambda 0})$ is the creation (annihilation) operator of the phonon of vibrational mode of multipolarity λ. The matrix elements of the rotational coupling operator ($\hat{O}_R$) between the $|n\rangle = |I0\rangle$ and $|m\rangle = |I'0\rangle$ states of the rotational band and the matrix elements of vibrational coupling operator ($\hat{O}_V$) between the n-phonon state $|n\rangle$ and the m-phonon state $|m\rangle$ are defined as

$$\hat{O}_{R(I,I')} = \sqrt{\frac{5(2I+1)(2I'+1)}{4\pi}}\beta_2 R_T \begin{pmatrix} I & 2 & I' \\ 0 & 0 & 0 \end{pmatrix}^2 + \sqrt{\frac{9(2I+1)(2I'+1)}{4\pi}}\beta_4 R_T \begin{pmatrix} I & 4 & I' \\ 0 & 0 & 0 \end{pmatrix}^2 \qquad (14)$$

and

$$\hat{O}_{V(nm)} = \frac{\beta_\lambda}{\sqrt{4\pi}} R_T(\delta_{n,m-1}\sqrt{m} + \delta_{n,m+1}\sqrt{n}) \qquad (15)$$

respectively. The Coulomb coupling matrix elements are computed by the linear coupling approximation and are defined as

$$V^C_{R(I,I')} = \frac{3Z_P Z_T R_T^2}{5r^3}\sqrt{\frac{5(2I+1)(2I'+1)}{4\pi}} \times \left(\beta_2 + \frac{2}{7}\beta_2^2\sqrt{\frac{5}{\pi}}\right)\begin{pmatrix} I & 2 & I' \\ 0 & 0 & 0 \end{pmatrix}^2 + \frac{3Z_P Z_T R_T^4}{9r^5}\sqrt{\frac{9(2I+1)(2I'+1)}{4\pi}} \times \left(\beta_4 + \frac{9}{7}\beta_2^2\right)\begin{pmatrix} I & 4 & I' \\ 0 & 0 & 0 \end{pmatrix}^2 \qquad (16)$$

and

$$V_{(C)}^{R(I,I')} = \frac{\beta_\lambda}{\sqrt{4\pi}} \frac{3}{2\lambda+1} Z_P Z_T e^2 \frac{R_T^\lambda}{r^{\lambda+1}} \times (\sqrt{m}\delta_{n,m-1} + \sqrt{n}\delta_{n,m+1}) \quad (17)$$

for the rotational and vibrational couplings respectively.

3. Results and Discussion

The present paper systematically analyzed the fusion dynamics of various heavy ion fusion reactions within the context of the static Woods-Saxon potential and energy dependent Woods-Saxon potential model along with Wong's approximation. The influences of nuclear structure degrees of freedom of the fusing pairs are investigated using the coupled channel calculations. In this work, the fusing systems are selected in such a way that the different projectiles: doubly magic ($^{16}_{8}$O), non-magic ($^{27}_{13}$Al) and semi-magic ($^{37}_{17}$Cl) nuclei are fused with the spherical Ge-isotopes ($^{70,72}_{32}$Ge). The values of the deformation parameters and corresponding excitation energies of low lying 2^+ and 3^- vibrational states of the colliding systems as required in the coupled channel calculations are listed in Table I. The barrier characteristics such as barrier height, barrier position and barrier curvature of various colliding pairs used in the EDWSP model calculations are listed in Table II. The potential parameter like range, depth and diffuseness parameters as used in the EDWSP model calculations for the chosen reactions are given in Table III.

The details of the coupled channel calculations for the fusion dynamics of $^{16}_{8}$O + $^{70,72}_{32}$Ge, $^{27}_{13}$Al + $^{70,72}_{32}$Ge and $^{37}_{17}$Cl + $^{70,72}_{32}$Ge reactions are shown in Fig. 3. The theoretical results based on the static Woods-Saxon potential and the energy dependent Woods-Saxon potential model (EDWSP model) along with the one dimensional Wong formula are depicted in Fig. 1. For all cases, the theoretical predations made by adopting the static Woods-Saxon potential along with one dimensional Wong formula are significantly smaller than the experimental data particularly at below barrier energies while at above barrier energies, experimental data has been properly accounted. The static Woods-Saxon potential produces single nominal barrier and therefore, theoretical calculations predict substantially small sub-barrier fusion cross-sections when compared with the experimental data. Such discrepancies between the theoretical predictions and the sub-barrier fusion data can be correlated with the nuclear structure degrees of freedom of the colliding systems like inelastic surface excitations. Quantitatively, one can overcome these deviations by including the influences of the dominant intrinsic channels in the coupled channel calculations (see Fig. 3). Alternatively, such discrepancies can be partially or fully overcome by introducing the energy dependence in the nucleus-nucleus potential in such a way that it becomes more attractive in the domain of the Coulomb barrier as compared to the standard Woods-Saxon potential. The enhanced attractive nature of the energy dependent Woods-Saxon potential lowers the fusion barrier and automatically predicts larger fusion excitation functions at sub-barrier energies. In EDWSP model based calculations, the reduction of the interaction barrier results in an adequate description of the observed fusion dynamics of the chosen reactions. Therefore, the barrier lowering effect is the main ingredient of the EDWSP model which in turn makes it an efficient theoretical tool to explore the heavy ion fusion reactions.

TABLE I. The deformation parameter (β_λ) and the energy (E_λ) of the quadrupole and octupole vibrational states of fusing nuclei.

Nucleus	β_2	E_2(MeV)	β_3	E_3(MeV)	Reference
$^{16}_{8}$O	0.370	6.920	0.700	6.130	[37]
$^{70}_{32}$Ge	0.230	1.040	0.230	2.560	[36-38]
$^{72}_{32}$Ge	0.250	0.830	0.240	2.510	[36-38]

TABLE II. The values of V_{B0}, R_B and $\hbar\omega$ used in the EDWSP model calculations for various heavy ion fusion reactions.

System	V_{B0}(MeV)	$R_B(fm)$	$\hbar\omega$(MeV)	Reference
$^{16}_{8}$O + $^{70}_{32}$Ge	35.17	9.76	3.40	[37]
$^{16}_{8}$O + $^{72}_{32}$Ge	35.00	9.81	3.20	[37]
$^{27}_{13}$Al + $^{70}_{32}$Ge	55.48	10.06	3.88	[36]
$^{27}_{13}$Al + $^{72}_{32}$Ge	54.81	10.20	3.85	[36]
$^{37}_{17}$Cl + $^{70}_{32}$Ge	68.74	10.66	3.74	[38]
$^{37}_{17}$Cl + $^{72}_{32}$Ge	68.43	10.71	3.71	[38]

TABLE III. Range, depth and diffuseness of the Woods-Saxon potential used in the EDWSP model calculations for various heavy ion fusion reactions [4,8-9,13,17-18,29-31].

System	$r_0(fm)$	V_0(MeV)	$\frac{a^{\text{Present}}}{\text{Enegy Range}}\left(\frac{fm}{\text{MeV}}\right)$
$^{16}_{8}$O + $^{70}_{32}$Ge	1.100	53.62	$\frac{0.95 \text{ to } 0.85}{28 \text{ to } 60}$
$^{16}_{8}$O + $^{72}_{32}$Ge	1.100	55.12	$\frac{0.95 \text{ to } 0.85}{28 \text{ to } 60}$
$^{27}_{13}$Al + $^{70}_{32}$Ge	1.090	76.20	$\frac{0.96 \text{ to } 0.85}{45 \text{ to } 65}$
$^{27}_{13}$Al + $^{72}_{32}$Ge	1.090	78.44	$\frac{0.96 \text{ to } 0.85}{45 \text{ to } 65}$
$^{37}_{17}$Cl + $^{70}_{32}$Ge	1.110	94.34	$\frac{0.96 \text{ to } 0.85}{60 \text{ to } 80}$
$^{37}_{17}$Cl + $^{72}_{32}$Ge	1.110	97.19	$\frac{0.95 \text{ to } 0.85}{28 \text{ to } 60}$

The energy dependence in the Woods-Saxon potential modifies the barrier characteristics of the interaction barrier between the colliding systems which in turn results in a spectrum of the variable fusion barriers as shown in Fig. 2. The spectrum of the energy dependent fusion barrier is shown for the $^{16}_{8}$O + $^{70}_{32}$Ge, $^{27}_{13}$Al + $^{70}_{32}$Ge and $^{37}_{17}$Cl + $^{70}_{32}$Ge reactions and the similar results are found for other projectile-target combinations. At below barrier energies, the largest diffuseness parameter ($a = 0.95fm$ for the $^{16}_{8}$O + $^{70}_{32}$Ge reaction, $a = 0.96fm$ for the $^{16}_{8}$O + $^{70}_{32}$Ge and $^{37}_{17}$Cl + $^{70}_{32}$Ge reactions) produces a lowest fusion barrier between the fusing systems. At this diffuseness, the lowest fusion barrier for $^{16}_{8}$O + $^{70}_{32}$Ge system is 33.95 MeV (for the $^{27}_{13}$Al + $^{70}_{32}$Ge reaction,

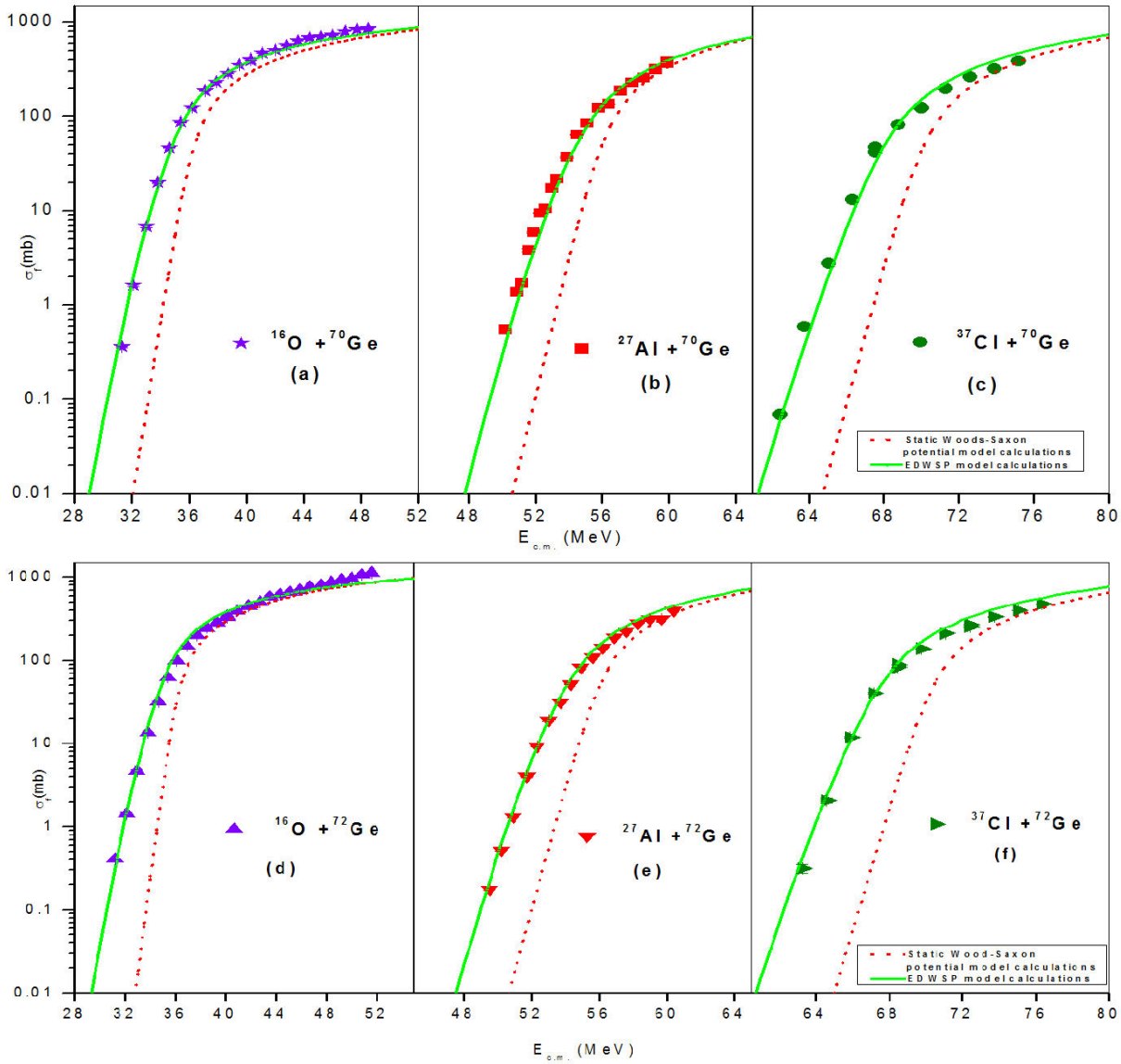

FIGURE 1. The fusion excitation functions of $^{16}_{8}$O + $^{70,72}_{32}$Ge, $^{27}_{13}$Al + $^{70,72}_{32}$Ge and $^{37}_{17}$Cl + $^{70,72}_{32}$Ge reactions obtained using the static Woods-Saxon potential model and the energy dependent Woods-Saxon potential model (EDWSP model). The fusion cross-sections ($\sigma_f(mb)$ are obtained using the EDWSP model (solid green line) and static Woods-Saxon potential (dotted red line) along with the Wong's approximation. The results are compared with the available experimental data taken from Ref. 36 to 38.

$FB = 53.20$ MeV and for $^{37}_{17}$Cl + $^{70}_{32}$Ge reaction, $FB = 66.20$ MeV). This fusion barrier is smaller than the Coulomb barrier by an amount of 1.22 MeV for $^{16}_{8}$O + $^{70}_{32}$Ge system (2.28 Mev for the $^{27}_{13}$Al + $^{70}_{32}$Ge and 2.54 MeV for the $^{37}_{17}$Cl + $^{70}_{32}$Ge systems) and hence the greater barrier modifications are required to address the observed fusion data of the chosen reactions. The presence of such fusion barrier physically accounts for the passage of the maximum flux from the incoming channel to fusion channel.

At above barrier energies, the fusion cross-sections are less sensitive towards nuclear structure as well as the channel coupling effects and consequently saturate at above barrier energies. This physical effect is properly modeled in the present approach wherein the magnitude of the diffuseness parameter gets saturated to its lowest value ($a = 0.85fm$) at above barrier energies. At well above the barrier, the highest fusion barrier for the $^{16}_{8}$O + $^{70}_{32}$Ge system is 35.05 MeV (for the $^{27}_{13}$Al + $^{70}_{32}$Ge reaction, $FB = 54.75$ MeV and for the $^{37}_{17}$Cl + $^{70}_{32}$Ge reaction, $FB = 68.15$ MeV). This fusion barrier is still smaller than the corresponding value of the Coulomb barrier as given in Table II. Therefore, the EDWSP model based calculation and the coupled channel calculation reasonably explored the fusion dynamics of the chosen reactions in quantitative as well as the qualitative way and henceforth, indicates that these theoretical methods produce analogous modifications in the barrier characteristics (barrier height, barrier position, barrier curvature) of the interaction fusion barrier between the colliding systems.

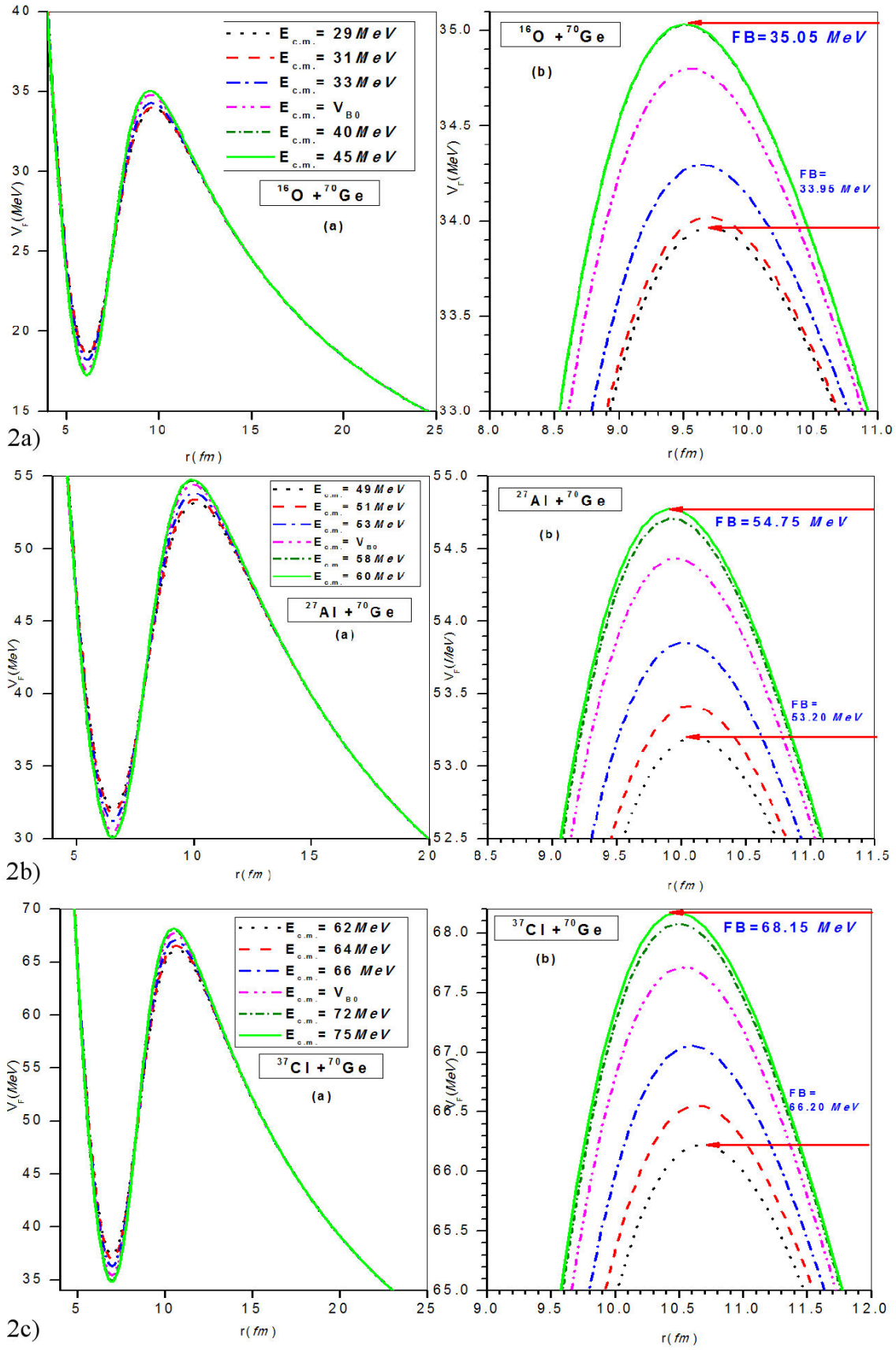

FIGURE 2. The fusion barrier (FB) for the $^{16}_{8}$O + $^{70}_{32}$Ge (Fig. 2a), $^{27}_{13}$Al + $^{70}_{32}$Ge (Fig. 2b) and $^{37}_{17}$Cl + $^{70}_{32}$Ge reactions (Fig. 2c) obtained using the EDWSP model. The similar results are found for other fusing systems.

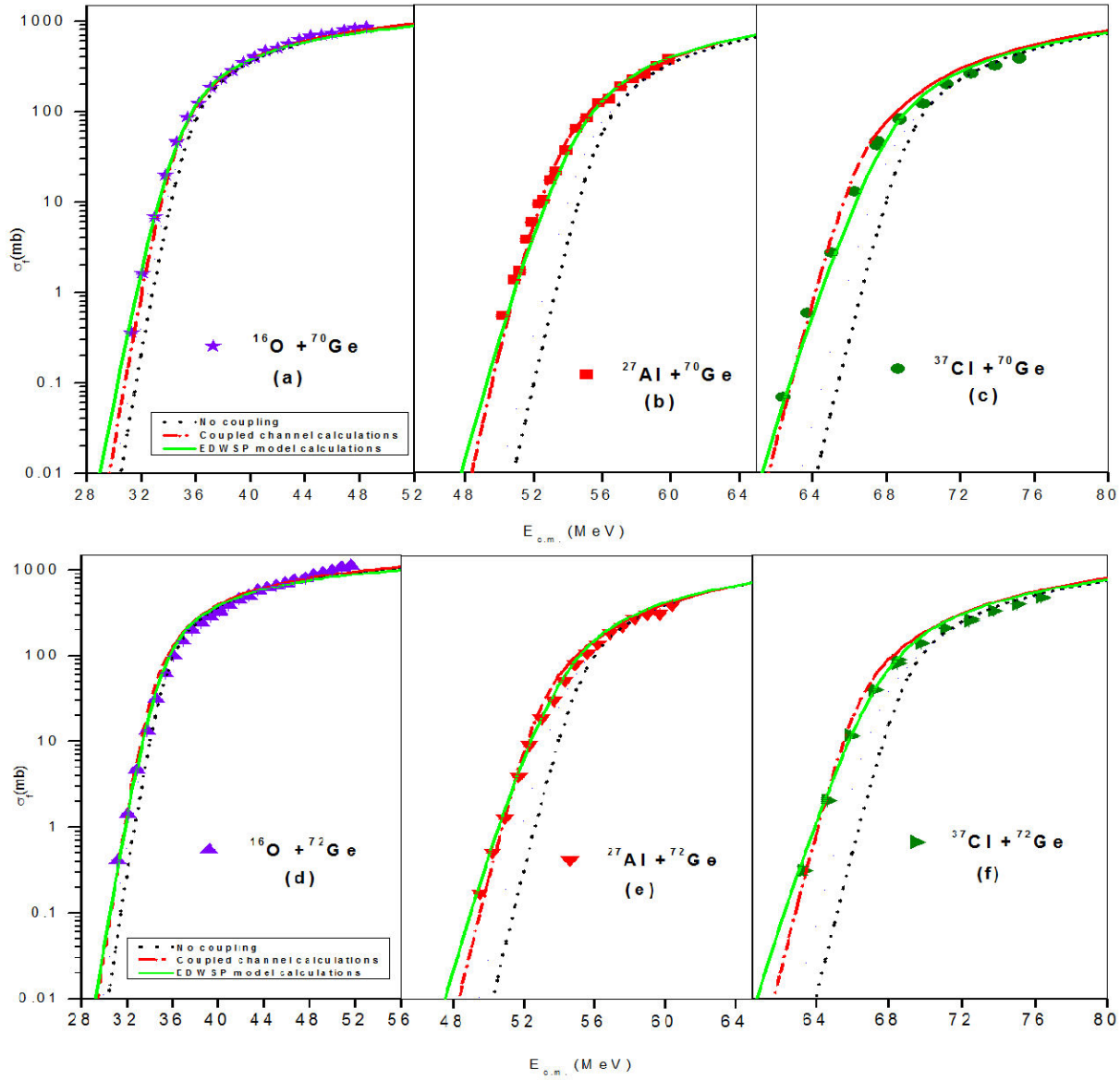

FIGURE 3. The fusion excitation functions of ${}^{16}_{8}\mathrm{O} + {}^{70,72}_{32}\mathrm{Ge}$, ${}^{27}_{13}\mathrm{Al} + {}^{70,72}_{32}\mathrm{Ge}$ and ${}^{37}_{17}\mathrm{Cl} + {}^{70,72}_{32}\mathrm{Ge}$ reactions obtained using the EDWSP model in conjunction with one dimensional Wong formula and the coupled channel code CCFULL. The fusion cross-sections ($\sigma_f(mb)$ obtained using the EDWSP model along with the Wong's approximation are shown by solid green line and the fusion cross-sections ($\sigma_f(mb)$ obtained through the static Woods-Saxon potential in the code CCFULL are denoted by dotted black line and dashed red line. The results are compared with the available experimental data taken from Ref. 36 to 38.

Morton *et al*. [50] suggested the weak influence of the collective vibrations of the ${}^{16}_{8}$O-isotope on fusion process but in the presence of strong channel coupling effects; it is very difficult to signify the importance of such weaker couplings. However, the Ge-isotope lies in the region of weak coupling and one can unambiguously identified the importance of the collective vibrations of ${}^{16}_{8}$O-isotope on fusion process. In the fusion of ${}^{16}_{8}\mathrm{O} + {}^{70,72}_{32}\mathrm{Ge}$ reaction, the projectile is doubly magic nucleus and facilitates the couplings to low lying inelastic surface excitations but due to high excitation energies of collective surface vibrational states, it weakly contributes to fusion process. In contrast, the inelastic surface excitations of the target isotope play very crucial role in the enhancement of the sub-barrier fusion cross-section of the chosen reactions with reference to the expectations of the one dimensional barrier penetration model. In coupled channel analysis, no coupling calculations, wherein the collision partners are taken as inert systems, quantitatively fail to account for the observed fusion enhancement particularly at below barrier energies. However, the above barrier fusion data is reasonably recovered by such coupling scheme. The addition of the one phonon 2^+ vibrational state of the target enhances the magnitude of the sub-barrier fusion excitation functions but unable to bring the required order of magnitude of the

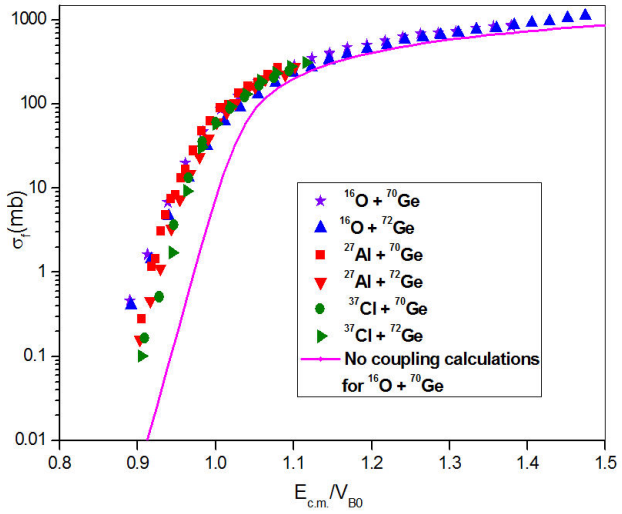

FIGURE 4. The fusion excitation functions data of ${}^{16}_{8}$O + ${}^{70,72}_{32}$Ge, ${}^{27}_{13}$Al + ${}^{70,72}_{32}$Ge and ${}^{37}_{17}$Cl + ${}^{70,72}_{32}$Ge reactions [36-38] has been compared in reduced scale.

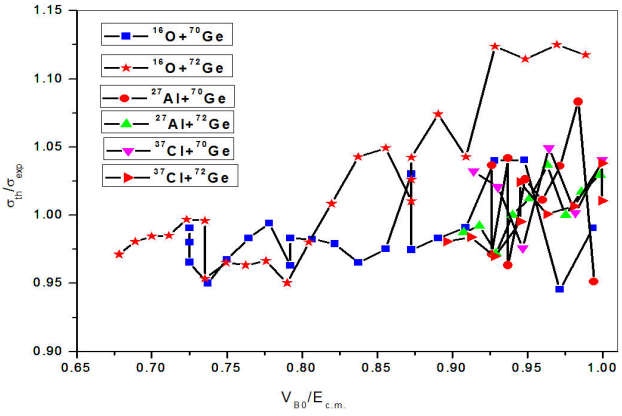

FIGURE 5. The ratio of $\xi = \sigma_{\rm th}/\sigma_{\rm exp}$ as the function of $V_{BO}/E_{c.m.}$ for 6 reactions listed in Table II.

sub-barrier fusion enhancement. This confirms the possible influences of the more intrinsic channels. The couplings to one phonon 2^+ and 3^- vibrational states of the target along with their mutual couplings considerably improve the theoretical results. However, the target degrees of freedom are not sufficient to properly explain the data and the additions of the projectile excitations are necessarily required to obtain the consistent fits with the experimental data. To overcome small discrepancies between theoretical predictions and the below barrier fusion data, the projectile excitations have been included in the coupled channel calculations. Therefore, the couplings to one phonon 2^+ vibrational state of the projectile, one phonon 2^+ and 3^- vibrational states of the target along with their mutual couplings quantitatively address the observed fusion dynamics of ${}^{16}_{8}$O + ${}^{70}_{32}$Ge reaction as shown in Fig. 3a. The similar coupling scheme has been used in the coupled channel analysis of ${}^{16}_{8}$O + ${}^{72}_{32}$Ge reaction. In case of ${}^{16}_{8}$O + ${}^{72}_{32}$Ge reaction, the inclusion of the one phonon vibrational state of the projectile, one phonon 2^+ and 3^- vibrational states of the target along with their mutual couplings recovers the discrepancies between the theoretical calculations based on static Woods-Saxon potential along with one dimensional Wong formula and the experimental fusion data as depicted from Fig. 3d. On the other hand, the energy dependence in nucleus-nucleus potential lowers the fusion barrier between the colliding pairs and hence reasonably addresses the sub-barrier fusion enhancement of ${}^{16}_{8}$O + ${}^{70,72}_{32}$Ge reactions. This clearly suggested that the influences of the channel coupling effects can be properly accounted by introducing the energy dependence in nucleus-nucleus potential.

${}^{27}_{13}$Al isotope lies in the transition region between prolate (${}^{24}_{12}$Mg) and oblate shapes (${}^{28}_{14}$Si) [36-38,50-51]. The measurements on quadrupole moment and transition probability ($B(E2\uparrow)$) support the oblate deformed shape of ${}^{27}_{13}$Al-isotope in its ground state [36-38,52-55]. Furthermore, several authors based on equivalent spheres model have shown that the consideration of the oblate deformed shape for the projectile (${}^{27}_{13}$Al) provides good fit to the fusion data in the whole range of energy spread across the Coulomb barrier. In case of ${}^{27}_{13}$Al + ${}^{70}_{32}$Ge reaction, the projectile is non-magic but due to odd-A nature; it exhibits large number of low lying inelastic surface excitations [36]. The couplings to these intrinsic channels strongly alter the energy dependence of the fusion cross-sections at below barrier energies. All these odd-spin states are added as quadrature, which produces dominant effects and hence entertained in coupled channel calculations. The couplings to one phonon 2^+ or one phonon 3^- vibrational state of the target nucleus alone significantly enhances the magnitude of sub-barrier fusion excitation functions with respect to no coupling calculations but unable to recover the required order of magnitude of the observed fusion enhancement at sub-barrier energies. This suggested that more intrinsic channels must be included in the coupled channel calculations. The inclusion of the odd-spin states as a quadrature in projectile and one phonon 2^+ and 3^- vibrational states along with their mutual couplings in target nucleus bring the observed fusion enhancement of ${}^{27}_{13}$Al + ${}^{70}_{32}$Ge reaction as shown in Fig. 3b. The similar coupling scheme has been tested for the coupled channel analysis of ${}^{27}_{13}$Al + ${}^{72}_{32}$Ge reaction and hence such calculations adequately explained the sub-barrier fusion enhancement of the chosen reaction as depicted in Fig. 3e. In contrast, within the context of the EDWSP model based calculations, the modification of the barrier characteristics (barrier position, barrier height, barrier curvature) reduces the fusion barrier in closely similar way as done by the channel coupling effects and hence accurately explained the fusion dynamics of ${}^{27}_{13}$Al + ${}^{70,72}_{32}$Ge reactions.

The theoretical results of the fusion dynamics of ${}^{37}_{17}$Cl + ${}^{70,72}_{32}$Ge reactions have the close resemblance to that of ${}^{27}_{13}$Al + ${}^{70,72}_{32}$Ge reactions. In the fusion of reaction, the projectile is magic but has moderate oblate deformed shape in its ground state. However, due to odd-A nature; it facilitates the addition of the large number of collective vibrational states. The couplings to these intrinsic channels strongly modify the energy dependence of the fusion cross-sections at below barrier

energies. All these odd-spin states are added as quadrature in coupled channel calculations [38] and hence significantly enhance the magnitude of the sub-barrier fusion excitation functions. In the fusion of $^{37}_{17}$Cl + $^{70}_{32}$Ge reaction, the low lying vibrational states of the projectile ($^{37}_{17}$Cl) produce dominant effects in enhancing the sub-barrier fusion excitation function with respect to the predictions of the one dimensional barrier penetration model. The addition of the one phonon 2^+ or one phonon 3^- vibrational state of the target nucleus alone is insufficient to account the experimental data at sub-barrier energies. This demands the couplings to more intrinsic channels for the complete description of the fusion data. The inclusion of the one phonon 2^+ and 3^- vibrational states in target as well as odd-A spin states in projectile along with their mutual couplings reasonably reproduces the observed fusion enhancement of $^{37}_{17}$Cl + $^{70,72}_{32}$Ge reaction in whole range of energy as shown in Fig. 3c. The similar coupling scheme has been used for the coupled channel description of $^{37}_{17}$Cl + $^{72}_{32}$Ge reaction wherein such calculations quantitatively recover the required order of the sub-barrier fusion enhancement as depicted in Fig. 3f. Interestingly, within the context of the EDWSP model based calculations, the barrier lowering effects decreases the interaction barrier between the collision partners in closely similar way as observed in the usual coupled channel approach and hence quantitatively reproduce the fusion dynamics of $^{37}_{17}$Cl + $^{70,72}_{32}$Ge reactions.

In Fig. 4, a comparison of the fusion excitation function data of $^{16}_{8}$O + $^{70,72}_{32}$Ge, $^{27}_{13}$Al + $^{70,72}_{32}$Ge and $^{37}_{17}$Cl + $^{70,72}_{32}$Ge reactions is shown in reduced scale. The subtle difference in the energy dependence of fusion cross-section at near and sub-barrier energies can be understood in terms of the collective surface vibrations of the target isotopes. The coupling strengths and the corresponding excitation energy of the octupole vibrational states of the target isotopes are almost same, however, the quadrupole vibrational states of the heavier target ($^{72}_{32}$Ge) lies at lower excitation energy which in turn displays the dominant effects relative to its quadrupole couplings. One expects a strong isotopic dependence of the sub-barrier fusion enhancement of $^{16}_{8}$O + $^{72}_{32}$Ge reaction with reference to the $^{16}_{8}$O + $^{70}_{32}$Ge reaction and also expects similar results for other fusing systems. However, instead of giving strong sub-barrier fusion enhancement, the chosen reactions show a weak isotopic dependence of the observed fusion dynamics as shown in Fig. 4.

The different kinds of channel coupling effects display their signature on the fusion excitation functions at sub-barrier energies while such physical effects have negligible influence on the above barrier fusion data. Therefore, the one dimensional barrier penetration model should provide a good description of the fusion data at above barrier energies. In this sense, a comparison of above barrier fusion data and the predictions of the present model for the fusion of $^{16}_{8}$O + $^{70,72}_{32}$Ge, $^{27}_{13}$Al + $^{70,72}_{32}$Ge and $^{37}_{17}$Cl + $^{70,72}_{32}$Ge reactions are shown in Fig. 5. Within EDWSP model, only at 7 fusion data points out of 77 fusion data points deviation exceed 5% whereas 70 fusion data points lie within 5%. Therefore, the EDWSP model is able to account the fusion data at above barrier energies within 5% with a probability greater than 90%. It is well accepted that the channel coupling effects lead to the barrier modifications effects and replace the single Coulomb barrier into a distribution of barriers of different height and weight. This barrier distribution is the mirror image of the type of coupling involved in the fusion enhancement at near and sub-barrier energies. In the same analogy, the EDWSP model induces barrier modification effects (barrier height, barrier position, barrier curvature) as depicted in Fig. 2. Therefore, as a consequence of the barrier lowering effects, the EDWSP model predicts substantially large fusion enhancement at below barrier energies and hence reasonably describe the observed fusion dynamics of the chosen reactions.

4. Conclusions

The present work analyzed the role of collective excitations of the fusing systems on the fusion mechanism of $^{16}_{8}$O + $^{70,72}_{32}$Ge, $^{27}_{13}$Al + $^{70,72}_{32}$Ge and $^{37}_{17}$Cl + $^{70,72}_{32}$Ge reactions. The theoretical calculations of the fusion excitation functions are performed using the static Woods-Saxon potential model and the EDWSP model along with Wong's approximation and the coupled channel calculations are performed using the code CCFULL. The theoretical predictions based on the static Woods-Saxon potential along with Wong formula substantially smaller than the experimental data. However, one can overcome such discrepancies by including the influences of the nuclear structure degrees of freedom associated with the colliding nuclei such as inelastic surface excitations. On the other hand, the EDWSP model along with one dimensional Wong formula provides the complete description of the observed fusion dynamics of $^{16}_{8}$O + $^{70,72}_{32}$Ge, $^{27}_{13}$Al + $^{70,72}_{32}$Ge and $^{37}_{17}$Cl + $^{70,72}_{32}$Ge reactions. In EDWSP model calculations, the energy dependence in nucleus-nucleus potential introduces the barrier modification effects (barrier height, barrier position, barrier curvature) and consequently reduces the height of fusion barrier between the colliding systems. This kind of barrier lowering effect increases the efficiency of the present model which in turn adequately explained the observed fusion enhancement of the various heavy ion fusion reactions. In addition, the EDWSP model is able to recover the above barrier fusion data within 10% and hence, the present approach reproduces the fusion cross-section data within 5% with a probability greater than 90%.

Acknowledgments

This work has been supported by Dr. D.S. Kothari Post-Doctoral Fellowship Scheme sponsored by University Grants Commission (UGC), New Delhi, India.

1. A.B. Balantekin and N. Takigawa, *Rev. Mod. Phys*. **70** (1998) 77.
2. L.F. Canto *et al*., *Phys. Rep*. **424** (2006) 1.
3. B.B. Back *et al*., *Rev. Mod. Phys*. **86** (2014) 317.
4. M.S. Gautam, *Nucl. Phys. A* **933** (2015) 272.
5. J.R. Leigh *et al*., *Phys. Rev. C* **52** (1995) 3151.
6. M. Dasgupta *et al*., *Annu. Rev. Nucl. Part. Sci*. **48** (1998) 401.
7. L.C. Vaz, *Comput. Phys. Commun*. **22** (1981) 451.
8. M.S. Gautam, *Mod. Phys. Lett. A* **30** (2015) 1550013.
9. M.S. Gautam, *Phys. Scr.* **90** (2015) 025301, *Phys. Scr*. **90** (2015) 055301, *Phys. Scr.* **90** (2015) 125301.
10. N. Wang and W. Scheid, *Phys. Rev. C* **78** (2008) 014607.
11. O.N. Ghodsi and R. Gharaei, *Eur. Phys. J. A* **48** (2012) 21.
12. W.D. Myers and W. J. Swaitecki, *Phys. Rev. C* **62** (2000) 044610
13. M.S. Gautam, *Acta Phys. Pol. B* **46** (2015) 1055.
14. R.N. Sagaidak *et al*. *Phys. Rev. C* **76** (2007) 034605.
15. O.N. Ghodsi and V. Zanganeh, *Nucl. Phys. A* **846** (2010) 40.
16. L.C. Chamon *et al*., *Phys. Rev. C* **66** (2002) 014610.
17. M.S. Gautam, *Can J. Phys*. **93** (2015) 1343; Pramana **86** (2016) 1067 *Chinese J. Phys.* **54** (2016) 86.
18. M.S. Gautam, *Chinese Phys. C* **39** (2015) 114102; *Chinese Phys. C* **40** (2016) 054101.
19. H. Esbensen *et al*., *Phys. Rev. C* **82** (2010) 054621.
20. A.M. Stefanini *et al*., *Phys. Lett. B* **679** (2009) 95.
21. J.O. Newton *et al*., *Phys. Rev. C* **70** (2004) 024605.
22. K. Hagino and N. Rowley, *Phys. Rev. C* **69** (2004) 054610.
23. A. Mukherjee *et al*., *Phys. Rev. C* **75** (2007) 044608.
24. A.M. Stefanini *et al*., *Phys. Rev. Lett.* **79** (1997) 5218.
25. K. Washiyama and D. Lacroix, *Phys. Rev. C* **74** (2008) 024610.
26. C. Simenel *et al*., *Phys. Rev. C* **88** (2013) 064604.
27. A.S. Umar *et al*., *Phys. Rev. C* **89** (2011) 034611.
28. A.S. Umar and V.E. Oberacker, *Eur. Phys. J. A* **39** (2009) 243.
29. M. Singh, Sukhvinder and R. Kharab, *Mod. Phys. Lett. A* **26** (2011) 2129, *Nucl. Phys. A* **897** (2013) 179, *Nucl. Phys. A* **897** (2013) 198, *AIP Conf. Proc*. **1524** (2013) 163, *EPJ Web of Conferences* **66** (2014) 03043.
30. M.S. Gautam, *Phys. Rev. C* **90** (2014) 024620, *Commun. Theor. Phys*. **64** (2015) 710, *Indian J. Phys*. **90** (2016) 335, *Braz. J. Phys*. **46** (2016)143.
31. M.S. Gautam *et al*., *Phys. Rev. C* **92** (2015) 054605, *AIP Conf. Proc.* **1675** (2015) 020052, Braz. *J. Phys*. **46** (2016)133.
32. D.W. Grissmer *et al*., *Nucl. Phys. A* **196** (1972) 216.
33. M.E. Cobern *et al.*, *Phys. Rev. C* **13** (1976) 674.
34. M.E. Cobern *et al*., *Phys. Rev. C* **13** (1976) 1200.
35. R. Lecomte *et al*., *Phys. Rev. C* **22** (1980) 1530.
36. E.F. Aguilera *et al*., *Phys. Rev. C* **41** (1990) 910.
37. E.F. Aguilera *et al*., *Phys. Rev. C* **52** (1995) 3103.
38. E.M. Quiroz *et al*., *Phys. Rev. C* **63** (2001) 054611.
39. H. Esbensen, *Phys. Rev. C* **68** (2003) 034604.
40. H. Esbensen, *Phys. Rev. C* **72** (2005) 054607.
41. Z.F. Muhammad *et al*., *Phys. Rev. C* **81** (2010) 044609.
42. H.M. Jia, *Phys. Rev. C* **86** (2012) 044621.
43. C.Y. Wong, *Phys. Rev. Lett*. **31** (1973) 766.
44. K. Hagino, N. Rowley and A.T. Kruppa, *Comput. Phys. Commun*. **123** (1999) 143.
45. D.L. Hill and J.A. Wheeler, *Phys. Rev*. **89** (1953) 1102.
46. K. Hagino *et al*., *Phys. Rev. C* **57** (1998) 1349.
47. Z.F. Muhammad *et al*., *Phys. Rev. C* **77** (2008) 014606.
48. K. Hagino and N. Takigawa, *Prog. Theor. Phys*. **128** (2012) 1061.
49. E.F. Aguilera and J.J. Kolata, *Phys. Rev. C* **85** (2012) 014603.
50. C.R. Morton *et al*., *Phys. Rev. Lett*. **74** (1994) 4074.
51. V.D. Luex *et al*., *Nucl. Phys. A* **100** (1967) 316.
52. D. Dehnard *et al*., *Phys. Lett. B* **38** (1972) 389.
53. R. Weber *et al*., *Nucl. Phys. A* **377** (1982) 361.
54. D. Schwalm *et al*., *Nucl. Phys. A* **239** (1977) 425.
55. D. Evers *et al*., *Nucl. Phys. A* **91** (1967) 472.